

Variable-time-delay optical coherent transient signal processing

K. D. Merkel and W. R. Babbitt

Department of Physics, Montana State University, Bozeman, Montana 59717-3840

K. E. Anderson and K. H. Wagner

Department of Electrical Engineering, University of Colorado, Boulder, Boulder, Colorado 80309

Received June 3, 1999

A technique is proposed and experimentally demonstrated that achieves simultaneous optical pattern waveform storage and programmable time delay for continuous real-time signal processing by use of optical coherent transient technology. We achieve variable-time-delay and broadband signal processing by frequency shifting of two chirped programming pulses, the chirp rate of one being twice that of the other, without using brief reference pulses and without changing the timing of the programming sequence. We demonstrate the technique experimentally in Tm^{3+} :YAG at 5 K for 40-MHz chirps by performing temporal signal convolution with true-time delays that vary over a 250-ns range. © 1999 Optical Society of America

OCS codes: 070.6020, 060.1660, 190.2640, 320.1590.

An optical coherent transient (OCT) signal processor¹⁻³ and an OCT variable true-time-delay (TTD) device⁴ have been proposed and demonstrated. After a brief review, we propose and experimentally demonstrate a novel method for simultaneously performing programmable time delay and optical signal processing for a continuous optical waveform modulated in amplitude and (or) phase at data rates greater than 10 GHz and with time-bandwidth products greater than 10,000.²

Previously proposed OCT devices store the spectral-spatial interference of two optical pulses separated in time as a population grating on an inhomogeneously broadened transition (IBT),¹⁻⁶ which can then process, or spectrally filter, a subsequently applied continuous data waveform.² One can store a pattern waveform in a grating by interfering it with a brief reference pulse (BRP). For optimal grating efficiency, the duration and intensity of a BRP should be sufficient to excite half of the atoms within the pattern and data bandwidth. To meet this constraint, the intensity of a BRP increases with bandwidth squared, so at wide bandwidths the appropriate intensities [$\sim 100 \text{ GW/cm}^2$ for 30 GHz in Tm :YAG (0.1 at. %)] are impractical to produce and can be of the order of the material bulk damage threshold. OCT signal processing can be achieved by an alternative technique in which the BRP is replaced with two frequency-chirped pulses, where the chirp rate of one pulse is twice that of the other.⁷ One advantage of chirped-pulse programming is the ability to store an optimally efficient grating with significantly lower pulse intensities than that of a BRP.

For processing received signals in an array of antennas,⁸ both variable TTD and signal processing are required. The previously demonstrated OCT TTD device achieved variable delay but not signal processing.⁴ In the typical OCT processor, variable delay is achieved only by external generation of a time difference between programming pulses. In this Letter we propose and demonstrate the use of frequency shifting of chirped pulses in an OCT signal processor to achieve variable time delay.

Four methods for achieving OCT signal processing with two frequency-chirped pulses, the chirp rate of one pulse being twice that of the other, in place of a BRP were presented in Ref. 7. We propose that, in all four cases, the use of frequency shifting to vary the stored time delay is possible. Of the two methods that were experimentally demonstrated in Ref. 7, that of reversed dephasing (convolution) is better at minimizing the coherence dephasing time between chirps than that of delayed rephasing (correlation). For this reason, only reversed dephasing is discussed and experimentally demonstrated here, but the analysis of this case can be extended to the other three methods for using frequency shifting to achieve time-delay variations for signal processing.

Programming an OCT processor without chirped pulses is typically achieved with two temporally modulated noncollinear optical pulses separated in time and resonant with an IBT. Each laser pulse has a form $E_n(t - t_n - \eta_n)\cos[\omega_0(t - \eta_n)]$, where the subscript n determines the order of arrival of each pulse, $E_n(\tau)$ is a slowly varying temporal envelope function, $\omega_0 = 2\pi\nu_0$ is the laser center frequency, $\eta_n = (\hat{k}_n \cdot \mathbf{r}/c)$, where \hat{k}_n is the unit wave vector of pulse n , and each pulse reaches the input face of the medium at $\hat{k}_n \cdot \mathbf{r} = 0$ at its arrival time t_n . Programming pulses $E_1(\tau)$ and $E_2(\tau)$, separated by $\tau_{21} = t_2 - t_1$, write a spatial-spectral holographic population grating on the IBT. After a grating is programmed, the atomic absorption is modulated in both frequency and space for subsequently applied optical waveforms. Within the grating lifetime, the application of $E_3(\tau)$ causes a coherent emission $E_S(t - t_S - \eta_S)\cos[\omega_0(t - \eta_S)]$ from the IBT with the temporal envelope of the form

$$E_S(t - t_S - \eta_S) \propto \int_{-\infty}^{\infty} E_1^*(\Omega)E_2(\Omega)E_3(\Omega) \times \exp[i\Omega(t - t_S - \eta_S)]d\Omega, \quad (1)$$

where $t_S = t_3 + t_2 - t_1$, $\eta_S = \eta_3 + \eta_2 - \eta_1$, and $E_n(\Omega)$ is the Fourier transform of the n th applied optical

waveform envelope, $E_n(\tau)$. Relation (1) is based on the Fourier-transform approximation of the input temporal waveforms,^{1,5} which is valid for waveforms with bandwidths less than the inhomogeneous linewidth and intensities that ensure a linear response and avoid both coherent and incoherent saturation.² Assuming that the input wave vectors are arranged to satisfy the phase-matching conditions, the output propagates with direction $\hat{k}_S = \hat{k}_3 + \hat{k}_2 - \hat{k}_1$.⁵ If $E_3(\tau)$ is a data waveform, the operation of correlation (convolution) between the pattern and data is achieved when the first (second) pulse is the pattern and the second (first) pulse is a BRP.

Figure 1 shows the four-pulse input sequence that we use to achieve convolution of a stored pattern waveform with a data waveform, using two chirped reference pulses and the physical process of reversed dephasing.⁷ The two chirps $E_{\text{chA}}(\tau)$ and $E_{\text{chB}}(\tau)$ have arrival times of t_{chA} and t_{chB} (defined here as the leading edge), durations τ_{chA} and $\tau_{\text{chB}} = 0.5\tau_{\text{chA}}$, respectively, and the same chirp bandwidth $\delta\nu_{\text{ch}}$. The vertical axes show the electric field amplitude of all pulses and the frequency of the chirped pulses (dashed lines). The pattern waveform is $E_P(\tau)$ at time t_P , and the data waveform is $E_D(\tau)$ at time t_D . In Fig. 1(b), the starting frequencies of the chirped pulses, ν_{S_A} and ν_{S_B} , respectively, are identical ($\nu_{S_A} = \nu_{S_B} = \nu_0 - \delta\nu_{\text{ch}}/2$) and linearly ramp over $\delta\nu_{\text{ch}}$ (to $\nu_0 + \delta\nu_{\text{ch}}/2$). In Fig. 1(b), the temporal separation between instantaneously identical frequencies is $\tau_{\text{chBA}} = t_{\text{chB}} - t_{\text{chA}}$, and these pulses cause a coherence at time $t_C = t_{\text{chB}} + \tau_{\text{chBA}} = 2t_{\text{chB}} - t_{\text{chA}}$,⁹ shown as the intersection of the dotted lines. This rephasing event can be predicted by the optical Bloch equations, the Fourier-transform approximation,⁵ the diagrammatic method,⁷ or a generalized perturbation theory.¹⁰

In terms of the traditional three-pulse sequence, the coherence at time t_C acts as $E_1(\tau)$ in Eq. (1), equivalent to a BRP, and the pattern waveform acts as $E_2(\tau)$.⁷ Therefore the stored TTD is $\tau_{\text{tttd}} = t_P - t_C$, and the emitted output signal occurs at time $t_S = t_D + (t_P - t_C) \equiv t_D + \tau_{\text{tttd}}$. The direction of the output signal is given by the six-wave mixing condition $\hat{k}_S = \hat{k}_{\text{chA}} - 2\hat{k}_{\text{chB}} + \hat{k}_P + \hat{k}_D$,⁷ with the same subscript notation. Even though this is a six-wave mixing process, the efficiency can ideally equal that of the typical OCT processor, which is a four-wave mixing process, when the intensities of the chirped pulses are optimized. Simulation results show that the efficiency is optimized when the Rabi frequencies Ω_{chA} and Ω_{chB} of the first and the second chirped pulses, respectively, are $\Omega_{\text{chA}} \approx 0.27(\delta\nu_{\text{ch}}/\tau_{\text{chA}})^{1/2}$ and $\Omega_{\text{chB}} \approx 4\Omega_{\text{chA}}$. In practice, the effects of propagation, absorption, coherence dephasing, and use of Gaussian beams will affect the optimization conditions, but the six- and four-wave mixing efficiencies should be of the same order.

The desired result is to vary the TTD that is programmed without changing the pulse timings or chirp bandwidths. Arbitrary control of t_C is possible by frequency shifting the chirped pulses. As t_C is determined by the temporal separation of identical frequencies between the two chirped pulses, a change in ν_{S_A}

and ν_{S_B} ($\delta\nu_{S_A}$ and $\delta\nu_{S_B}$, respectively) or of both translates to changing the effective time delay τ_{chBA} without actually changing ($t_{\text{chB}} - t_{\text{chA}}$). We define $\delta\nu_{S_{BA}} = \nu_{S_B} - \nu_{S_A}$; then $t_C = (2t_{\text{chB}} - t_{\text{chA}}) - \delta\nu_{S_{BA}}(\tau_{\text{chA}}/\delta\nu_{\text{ch}})$. A variation in t_C with a fixed t_P translates into a change in τ_{tttd} . As $E_{\text{chA}}(\tau)$ acts to first order and $E_{\text{chB}}(\tau)$ acts to second order, equally opposite values of $\delta\nu_{S_A}$ and (or) $\delta\nu_{S_B}$ have the same net result. For example, if $\tau_{\text{chA}} = 1.0 \mu\text{s}$ and $\delta\nu_{\text{ch}} = 40 \text{ MHz}$ (as in the experiment, below) then $t_C = (2t_{\text{chB}} - t_{\text{chA}}) - 125 \text{ ns}$ by (1) $\delta\nu_{S_A} = -5 \text{ MHz}$, $\delta\nu_{S_B} = 0$, (2) $\delta\nu_{S_A} = 0$, $\delta\nu_{S_B} = +5 \text{ MHz}$, or (3) $\delta\nu_{S_A} = -2.5 \text{ MHz}$, $\delta\nu_{S_B} = +2.5 \text{ MHz}$. Frequency shifting reduces the spectral overlap of the chirped pulses, so for a processing bandwidth $\delta\nu_{\text{proc}}$ the condition $|\delta\nu_{S_{BA}}| \leq (\delta\nu_{\text{ch}} - \delta\nu_{\text{proc}})$ should be satisfied. Optimally, equal and opposite shifts about ν_0 (or the frequency-shifting device offset) are used. Figure 1(a) [Fig. 1(c)] shows the effect of a shorter (longer) stored delay τ_{tttd} (τ_{tttd}') by equal and opposite values of $\delta\nu_{S_A}$ and $\delta\nu_{S_B}$, such that $\delta\nu_{S_{BA}}$ is negative (positive) without any change in the input sequence timing. The maximum delay tuning range by frequency shifting is $\pm(\delta\nu_{\text{ch}} - \delta\nu_{\text{proc}})(\tau_{\text{chA}}/\delta\nu_{\text{ch}})$.

Frequency-tuned TTD optical signal processing was experimentally demonstrated in a 1.0-mm-long $\text{Tm}^{3+}:\text{YAG}$ crystal (0.5 at. %), maintained at 5 K. The continuous-wave output of an argon-pumped Ti:sapphire laser, resonant with the 793-nm transition¹¹ of Tm^{3+} , was crafted into optical pulses by

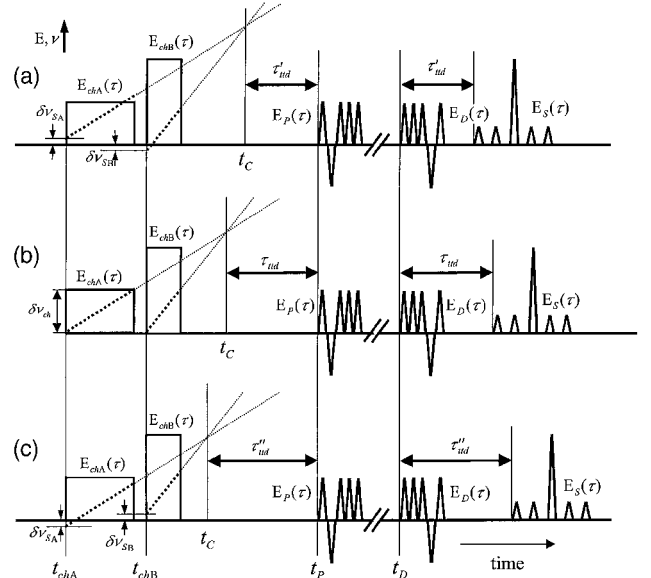


Fig. 1. Four-pulse input sequence to achieve convolution and variable time delay by application of two frequency chirps, a pattern and a data waveform. Vertical axes, electric field amplitude of all pulses and also frequencies of chirped pulses (bold dashed lines). In (b), both starting frequencies of the chirps are identical, causing a coherence at t_C (intersection of the dotted lines). In (a) [(c)] the coherence caused by the two chirps occurs later [earlier] because of frequency shifting. The net result is to vary the time delay stored along with the pattern waveform, $\tau_{\text{tttd}} = t_P - t_C$, without changing the timing of the input sequence. In all three cases the signal $E_S(\tau)$ (not to scale) is the convolution of the pattern and data waveforms emitted after the appropriate delay.

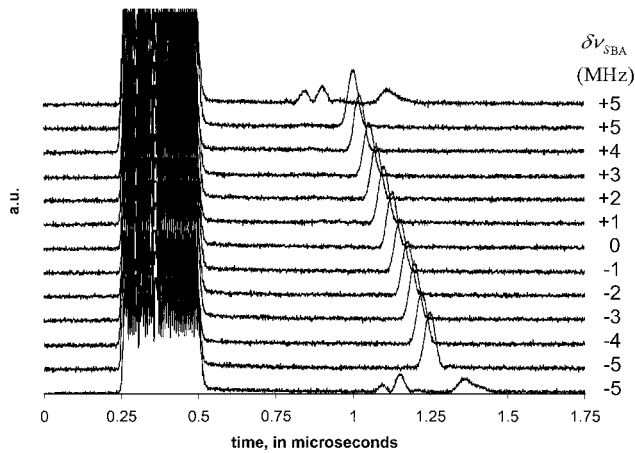


Fig. 2. Experimental output data showing variable time delay and signal processing by frequency tuning of the chirped pulses. With reference to the data waveform (left), the time delay of the emitted signal (0.75–1.0 μ s) varies with the offsets of the chirp frequencies $\delta\nu_{SBA}$. The 11 peaks are the detected intensity of the emitted signals representing the autocorrelation of the code; in addition, two other signals are shown, at $\delta\nu_{SBA} = \pm 5$ MHz, representing the autoconvolution of the code.

a 40-MHz acousto-optic modulator driven by a 1-GHz arbitrary waveform generator that controlled the amplitude, frequency, and phase of all the input pulses. Two identical acousto-optic modulators deflected different portions of this pulse sequence onto separate beams, preserving the frequency relationships between pulses. The two beams were focused (100- μ m $1/e^2$ diameter spot) and crossed in the crystal. The output waveforms were incident onto an 800-MHz avalanche photodetector and were captured single shot (every 50 ms) by a 1.0-GHz digitizing oscilloscope.

A standard programming waveform sequence was chosen to maximize the amplitude of the emitted signal without saturating the transition of interest within the experimental constraints. The two frequency-chirped pulses had peak powers of 70 and 100 mW (power limited) and durations of 1.0 and 0.5 μ s, respectively, and each was chirped over 40 MHz. The first chirp was on beam 1, and the second chirp was on beam 2. The timing ($t_{chB} - t_{chA}$) between the chirps was 1.368 μ s. Both the pattern pulse and the data stream occurred on beam 2 and were 5-bit biphasic nonreturn-to-zero codes, each bit of duration 50 ns with power 100 mW. The pattern occurred 1.4 μ s after the second chirp ended, and the data occurred 6.4 μ s after the pattern ended.

Figure 2 shows the experimental results that we achieved by keeping the timing of the input sequence fixed. For all cases we changed ν_{SB} and ν_{SA} in equal and opposite amounts of 0.5 MHz, so each increment of $\delta\nu_{SBA}$ was 1 MHz (25 ns). Delay tuning of ± 125 ns was achieved for $\delta\nu_{SBA}$ over a range of -5 to $+5$ MHz. The emitted output was detected along beam 1, and the maximum power of these signals was approximately 0.15 mW. Along beam 1 a small fraction (0.25%) of the data waveform (scattered from beam 2) was also detected and served as a reference, showing that the

signal was emitted after a variable programmed delay in each case. The operation in all cases was the convolution of the pattern and data waveforms. In the 11 peaks shown, the programmed pattern was a time-reversed replica of the data $\{+, +, +, -, +\}$, so the emitted output is the autocorrelation of the code. Two additional output signals are shown at $\delta\nu_{SBA} = \pm 5$ MHz, where the programmed pattern was identical to the data, resulting in the autoconvolution of the code.

These results show the emitted signal occurring at different times for the application of a common waveform applied to each channel at the same time. In a typical TTD receiver processor device a common data waveform arrives at different times (i.e., an angled wave front), and a frequency-tuned delay on each channel compensates for that difference while simultaneously correlating the wave front with the stored patterns. Additionally, continuous programming of the pattern and time delay¹² permits continuous processing by a steady-state grating or adaptive learning for varying incoming signals.

In summary, we have demonstrated a novel technique for programming a variable true-time delay and pattern waveform as a spectral-spatial population grating. Delays that varied over a 250-ns range were demonstrated without changes in the timing of the input pulse sequence. The demonstrated bandwidth was limited by the acousto-optic modulators, representing $\sim 0.1\%$ of the available 17-GHz bandwidth in Tm^{3+} :YAG. Chirped-pulse programming of optical coherent transient processors permits the design of a versatile, all-optical device for transmitting and processing of received signals in broadband array antennas.

We gratefully acknowledge the support of this research by the U.S. Army Research Office under Defense Experimental Program to Stimulate Competitive Research grant DAAG55-98-1-0244.

References

1. Y. S. Bai, W. R. Babbitt, N. W. Carlson, and T. W. Mossberg, *Appl. Phys. Lett.* **45**, 714 (1984).
2. W. R. Babbitt and J. A. Bell, *Appl. Opt.* **33**, 1538 (1994); M. Zhu, W. R. Babbitt, and C. M. Jefferson, *Opt. Lett.* **20**, 2514 (1995).
3. X. A. Shen, Y. S. Bai, and R. Kachru, *Opt. Lett.* **17**, 1079 (1992).
4. K. D. Merkel and W. R. Babbitt, *Opt. Lett.* **21**, 1102 (1996); **23**, 528 (1998).
5. T. W. Mossberg, *Opt. Lett.* **7**, 77 (1982).
6. M. Mitsunaga, R. Yano, and N. Uesugi, *Opt. Lett.* **16**, 1890 (1991).
7. K. D. Merkel and W. R. Babbitt, *Appl. Opt.* **35**, 278 (1996).
8. B. Widrow and S. D. Stearns, *Adaptive Signal Processing* (Prentice-Hall, Englewood Cliffs, N.J., 1985).
9. Y. S. Bai and T. W. Mossberg, *Appl. Phys. Lett.* **45**, 1269 (1984); *Opt. Lett.* **11**, 30 (1986).
10. M. Mitsunaga and R. G. Brewer, *Phys. Rev. A* **32**, 1605 (1985).
11. R. M. Macfarlane, *Opt. Lett.* **18**, 1958 (1993).
12. K. D. Merkel and W. R. Babbitt, *Opt. Lett.* **24**, 172 (1999).